


Quark quasi-Sivers function and quasi-Boer-Mulders function in a spectator diquark model

Chentao Tan and Zhun Lu^{*}*School of Physics, Southeast University, Nanjing 211189, China* (Received 23 June 2022; accepted 17 October 2022; published 3 November 2022)

We compute the leading-twist T-odd quasidistributions of the proton in a spectator model with scalar and axial-vector diquarks: the quasi-Sivers function $\tilde{f}_{1T}^\perp(x, \mathbf{k}_T^2; P_z)$ and the quasi-Boer-Mulders function $\tilde{h}_1^\perp(x, \mathbf{k}_T^2; P_z)$. We obtain the quark-quark correlators in the four-dimensional Euclidian space by replacing γ^+ and σ^{i+} in the light-cone frame with γ_z and σ_{iz} . We show by analytical calculation that the results of \tilde{f}_{1T}^\perp and \tilde{h}_1^\perp derived from the correlators can reduce to the expressions of the corresponding standard T-odd distributions $f_{1T}^\perp(x, \mathbf{k}_T^2)$ and $h_1^\perp(x, \mathbf{k}_T^2)$ in the limit $P_z \rightarrow \infty$. The numerical results for these quasidistributions and their first transverse moments for the u and d quarks in different x and P_z regions are also presented. We find that $\tilde{f}_{1T}^{\perp(1)}(x, P_z)$ and $\tilde{h}_1^{\perp(1)}(x, P_z)$ in the spectator model are fair approximations to the standard ones (within 20%–30%) in the region $0.1 < x < 0.5$ when $P_z \geq 2.5$ –3 GeV. This supports the idea of using T-odd quasidistributions to obtain standard distributions in the region $P_z > 2.5$ GeV as fair approximation.

DOI: [10.1103/PhysRevD.106.094003](https://doi.org/10.1103/PhysRevD.106.094003)

I. INTRODUCTION

The Parton distribution functions (PDFs), defined through the light-cone correlation functions are of fundamental importance in hadronic physics. They describe the density of a parton carrying in hadron a light-cone fraction x of the total momentum. Although PDFs are difficult to calculate from the first principle of QCD, they play a crucial role in the description of various high energy inclusive processes via the QCD factorization theorem. A natural extension of PDFs is the transverse-momentum-dependent distributions (TMDs) [1]. They encode the probability density of a parton inside the nucleon with longitudinal momentum fraction x and transverse momentum \mathbf{k}_T . In leading-twist there are eight TMDs, corresponding to different polarization states of the hadron and the parton. Of particular interest are two T-odd TMDs, namely, the Sivers function $f_{1T}^\perp(x, \mathbf{k}_T^2)$ and the Boer-Mulders function $h_1^\perp(x, \mathbf{k}_T^2)$. The former one describes the asymmetric distribution of the unpolarized parton in a transverse polarized hadron [2,3], while the latter one describes the distribution of the transverse polarized parton in an unpolarized hadron [4]. For these reasons

they can give rise to the spin or azimuthal asymmetries in a semi-inclusive deep inelastic scattering process or Drell-Yan process.

Recently, the concept of quasi-PDFs for hadrons has been proposed in Refs. [5,6] and has received a lot of attention. Different from the standard PDFs, quasi-PDFs are defined by the bilocal operators on a spatial interval such that they can be calculated by the lattice QCD in a four-dimensional Euclidian space. Quasi-PDFs have a parton probability interpretation similar to the standard PDFs, but for a parton carrying a fraction x of the finite momentum \vec{P} of the hadron. Although introducing quasi-PDFs will bring an explicit dependence on the hadron momentum (usually denoted by $P_z = |\vec{P}|$), it is found that, in the large limit of P_z , the quasi-PDF $\tilde{f}(x, P_z)$ converges to the standard PDF $f(x)$. This makes it possible to calculate the x dependence of the standard PDFs by using lattice QCD. In particular, a number of lattice calculations on quasi-PDFs and related quantities [7–27] have been performed.

The framework of the quasidistributions can be also extended to the case of TMDs, as already proposed in Ref. [5]. The quasi-TMD $\tilde{f}(x, \mathbf{k}_T^2; P_z)$ has a parton probability interpretation similar to the TMD, but is defined in the Euclidean space and depends on the hadron momentum P_z . In Refs. [28,29], the basic procedure that can be used to compute the TMDs from lattice QCD using large momentum effective theory (LAMET) [30] or quasi-TMDs has been laid out. The T-even spin-dependent quasi-TMDs that are amenable to lattice QCD calculations and that can be

*zhunlu@seu.edu.cn

Published by the American Physical Society under the terms of the [Creative Commons Attribution 4.0 International license](https://creativecommons.org/licenses/by/4.0/). Further distribution of this work must maintain attribution to the author(s) and the published article's title, journal citation, and DOI. Funded by SCOAP³.

used to determine standard spin-dependent TMDPDFs have also been constructed in Ref. [31]. Furthermore, the quark Sivers function is computed [32] in the leading-order expansion in the framework of LAMET.

In this work, we will study the quasidistributions of the T-odd TMDs from the model aspects. As demonstrated in Refs. [33–40], model calculations on quasidistributions can provide useful information for which values of P_z the quasi-PDFs are fair approximations of standard PDFs. To explore for what values of P_z the T-odd quasi-TMDs and the standard T-odd TMDs are approximations of each other, we calculate the quark quasi-Sivers function $\tilde{f}_{1T}^\perp(x, k_T^2; P_z)$ and quasi-Boer-Mulders function \tilde{h}_1^\perp using a spectator diquark model. We would like to study the flavor dependence of these quasidistributions; therefore, in the calculation we include both the scalar diquark and the axial-vector diquark to obtain the distributions of u and d quarks. In addition, we select the dipolar form factor for the proton-quark-diquark vertex.

This paper is organized as follows: In Sec. II, we present the definitions of standard T-odd TMDs and the corresponding quasi-TMDs by using the light-cone correlators and the Euclidean correlators, respectively. In Sec. III, we perform the calculations of two quasidistributions in the

spectator model with scalar and axial-vector diquarks. In Sec. IV, we give the numerical results for the quasifunctions and the first k_T -moment of two functions to explore the dependence of these distributions on x , P_z , and k_T . We provide some conclusions in Sec. V.

II. DEFINITION: STANDARD SIVERS FUNCTION AND BOER-MULDERS FUNCTION, QUASI-SIVERS FUNCTION AND QUASI-BOER-MULDERS FUNCTION

In this section, we present the operator definitions for the standard TMD distributions f_{1T}^\perp and h_1^\perp , as well as the quasi-TMD distributions \tilde{f}_{1T}^\perp and \tilde{h}_1^\perp , respectively.

The standard TMD distributions are usually expressed in the light-cone coordinate, in which one writes $a^\pm = (a^0 \pm a^3)/\sqrt{2}$ and $\mathbf{a}_T = (a_1, a_2)$ for an arbitrary four-vector a^μ in a specific reference frame, and the components of a^μ are given as (a^+, a^-, \mathbf{a}_T) . The standard TMD distributions for a quark with light-cone momentum fraction $x = k^+/P^+$ and transverse momentum \mathbf{k}_T appear in the decomposition of the quark-quark correlation function Φ (in deep inelastic scattering)

$$\Phi_{ij}(x, \mathbf{k}_T, S) = \int \frac{d\xi^- d^2\xi_T}{(2\pi)^3} e^{-i\xi \cdot k} \langle P, S | \bar{\psi}_j(0) \mathcal{U}^{n^-}[0, +\infty] \mathcal{U}^{n^-}[+\infty, \xi] \psi_i(\xi) | P, S \rangle_{\xi^+ = 0}, \quad (1)$$

which can be parametrized according to the hermiticity, parity invariance, and charge conjugation invariance. In the above equation, k^μ is the momentum of the quark, and

$$P^\mu = (P^+, P^-, \mathbf{0}_T), \quad S^\mu = \left(S_L \frac{P^+}{M}, -S_L \frac{P^-}{M}, \mathbf{S}_T \right) \quad (2)$$

are the momentum and the polarization vector of the nucleon, respectively. Furthermore, \mathcal{U}^{n^-} are the gauge links to ensure the gauge invariance of the operator definition,

$$\mathcal{U}^{n^-}[0, +\infty] = \mathcal{P} \exp \left[-ig \int_{0^-}^{\infty^-} d\eta^- A^+(0^+, \eta^-, \mathbf{0}_T) \right] \mathcal{P} \exp \left[-ig \int_{0_T}^{\infty_T} d\zeta_T \cdot A_T(0^+, \infty^-, \zeta_T) \right], \quad (3)$$

$$\mathcal{U}^{n^-}[+\infty, \xi] = \mathcal{P} \exp \left[-ig \int_{\xi_T}^{\infty_T} d\zeta_T \cdot A_T(0^+, \infty^-, \zeta_T) \right] \mathcal{P} \exp \left[-ig \int_{\xi^-}^{\infty^-} d\eta^- A^+(0^+, \eta^-, \xi_T) \right], \quad (4)$$

where $n^- = (0, 1, \mathbf{0}_T)$, and \mathcal{P} denotes all possible ordered paths followed by the gluon field A , which couples to the quark field ψ through the coupling constant g .

Then the standard Sivers function $f_{1T}^\perp(x, \mathbf{k}_T^2)$ and Boer-Mulders function $h_1^\perp(x, \mathbf{k}_T^2)$ can be defined by the following expressions [1]:

$$\frac{\epsilon_T^{ij} k_{Ti} S_{Tj}}{M} f_{1T}^\perp(x, \mathbf{k}_T^2) = -\frac{1}{4} \text{Tr}[\Phi^{[\gamma^+]}(x, \mathbf{k}_T, S) - \Phi^{[\gamma^+]}(x, \mathbf{k}_T, -S)] + \text{H.c.}, \quad (5)$$

$$\frac{\epsilon_T^{ij} k_{Ti}}{M} h_1^\perp(x, \mathbf{k}_T^2) = \frac{1}{4} \text{Tr}[\Phi^{[i\sigma^{i+}\gamma_5]}(x, \mathbf{k}_T, S) + \Phi^{[i\sigma^{i+}\gamma_5]}(x, \mathbf{k}_T, -S)] + \text{H.c.}, \quad (6)$$

where H.c. denotes the Hermitian conjugate terms, and

$$\Phi^{[\gamma^+]}(x, \mathbf{k}_T, S) = \frac{1}{2} \text{Tr}[\Phi(x, \mathbf{k}_T, S) \gamma^+], \quad (7)$$

$$\Phi^{[i\sigma^{i+}\gamma_5]}(x, \mathbf{k}_T, S) = \frac{1}{2} \text{Tr}[\Phi(x, \mathbf{k}_T, S) i\sigma^{i+}\gamma_5]. \quad (8)$$

On the other hand, quasi-TMDs are defined as the matrix elements of the following equal-time spatial correlation function [5]

$$\tilde{\Phi}_{ij}(x, \mathbf{k}_T, S; P_z) = \int \frac{d\xi^z d^2\xi_T}{(2\pi)^3} e^{-i\xi \cdot k} \langle P, S | \bar{\psi}_j(0) \mathcal{U}^{n_z}[0, +\infty] \mathcal{U}^{n_z}[+\infty, \xi] \psi_i(\xi) | P, S \rangle |_{\xi_0=0}, \quad (9)$$

where $x = k_z/P_z$ is the longitudinal momentum fraction of the quark, and $\mathcal{U}^{n_z}[0, +\infty]$ and $\mathcal{U}^{n_z}[+\infty, \xi]$ are the gauge links having the forms¹

$$\mathcal{U}^{n_z}[0, +\infty] = \mathcal{P} \exp \left[-ig \int_{0^z}^{\infty^z} d\eta^z A^z(0^0, \eta^z, \mathbf{0}_T) \right] \mathcal{P} \exp \left[-ig \int_{0_T}^{\infty_T} d\zeta_T \cdot A_T(0^0, \infty^z, \zeta_T) \right], \quad (10)$$

$$\mathcal{U}^{n_z}[+\infty, \xi] = \mathcal{P} \exp \left[-ig \int_{\xi_T}^{\infty_T} d\zeta_T \cdot A_T(0^0, \infty^z, \zeta_T) \right] \mathcal{P} \exp \left[-ig \int_{\xi^z}^{\infty^z} d\eta^z A^z(0^0, \eta^z, \xi_T) \right]. \quad (11)$$

Using the correlation function in Eq. (9), we can write the expressions for calculating the quasi-Sivers function $\tilde{f}_{1T}^\perp(x, \mathbf{k}_T^2, P_z)$ and the quasi-Boer-Mulders function $\tilde{h}_1^\perp(x, \mathbf{k}_T^2, P_z)$ as follows [5,33]:

$$\frac{\epsilon_T^{ij} \mathbf{k}_{Ti} S_{Tj}}{M} \tilde{f}_{1T}^\perp(x, \mathbf{k}_T^2, P_z) = -\frac{1}{4} \text{Tr}[\tilde{\Phi}^{[\gamma_z]}(x, \mathbf{k}_T, S) - \tilde{\Phi}^{[\gamma_z]}(x, \mathbf{k}_T, -S)] + \text{H.c.}, \quad (12)$$

$$\frac{\epsilon_T^{ij} \mathbf{k}_{Ti}}{M} \tilde{h}_1^\perp(x, \mathbf{k}_T^2, P_z) = \frac{1}{4} \text{Tr}[\tilde{\Phi}^{[i\sigma_{iz}\gamma_5]}(x, \mathbf{k}_T, S) + \tilde{\Phi}^{[i\sigma_{iz}\gamma_5]}(x, \mathbf{k}_T, -S)] + \text{H.c.}, \quad (13)$$

where $\tilde{\Phi}^{[\gamma_z]}$ and $\tilde{\Phi}^{[i\sigma_{iz}\gamma_5]}$ are defined as

$$\tilde{\Phi}^{[\gamma_z]}(x, \mathbf{k}_T, S) = \frac{1}{2} \text{Tr}[\tilde{\Phi}(x, \mathbf{k}_T, S; P_z) \gamma_z], \quad (14)$$

$$\tilde{\Phi}^{[i\sigma_{iz}\gamma_5]}(x, \mathbf{k}_T, S) = \frac{1}{2} \text{Tr}[\tilde{\Phi}(x, \mathbf{k}_T, S; P_z) i\sigma^{iz} \gamma_5]. \quad (15)$$

III. ANALYTIC CALCULATION

In this section, we present the analytic calculation of the quasi-Sivers function and the quasi-Boer-Mulders function using a spectator model.

The model has been widely used to calculate the standard TMDs [41–43] and generalized parton distributions (GPDs) of the nucleon and the spin-0 hadron. Recently, it was also applied to calculate quasi-PDFs [33] and quasi-GPDs [44–46]. In the model, the nucleon is viewed as a two-body composite system of an active quark with mass m and a diquark with mass M_X . The latter one can be a scalar

¹For a generic four-vector a^μ , we denote the ordinary Minkowski components by (a^0, \mathbf{a}_T, a^z) .

diquark or an axial-vector diquark according to its spin. As shown in Fig. (1), the proton-quark-diquark coupling is characterized by some effective vertices. For this purpose we adopt the vertices for the scalar and the axial-vector diquarks as

$$\text{scalar diquark: } ig_s(k^2), \quad (16)$$

$$\text{axial-vector diquark: } i \frac{g_a(k^2)}{\sqrt{2}} \gamma^\mu \gamma_5, \quad (17)$$

where $g_X(k^2)$ denotes the form factors of the coupling. In our calculations, we will use the dipolar form factor

$$g_X(k^2) = g_X \frac{k^2 - m^2}{|k^2 - \Lambda_X^2|^2} = g_X \frac{(k^2 - m^2)(1-x)^2}{(\mathbf{k}_T^2 + L_X^2(\Lambda_X^2))^2}, \quad (18)$$

where

$$L_X^2(\Lambda_X^2) = xM_X^2 + (1-x)\Lambda_X^2 - x(1-x)M^2, \quad (19)$$

with $(P-k)^2 = M_X^2$. g_X and Λ_X denote the coupling constants and the cutoffs, respectively. They are considered as the free parameters of the model together with the diquark mass M_X . In addition, the propagators of the scalar and axial-vector diquarks are given by

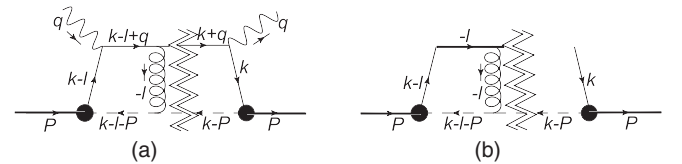


FIG. 1. (a) Interference between the one-gluon exchange diagram and the tree-level diagram in the spectator diquark model. (b) Interference between the one-gluon exchange diagram and the tree-level diagram in the spectator diquark model in eikonal approximation.

$$\text{scalar diquark: } \frac{i}{k^2 - M_s^2}, \quad (20)$$

$$\text{axial-vector diquark: } \frac{i}{k^2 - M_a^2} d^{\mu\nu}. \quad (21)$$

In this work, we adopt $d^{\mu\nu} = -g^{\mu\nu}$ to simplify the calculation. We admit that this polarization sum contains unphysical polarization states of the axial-vector diquark.

A. Standard Sivers function and Boer-Mulders function

The quark Sivers function and quark Boer-Mulders function have been calculated by various models in the literature, such as the spectator model [43,47–52], light-cone quark model [41,53], nonrelativistic constituent quark model [54,55], and MIT bag model [55–57]. In order to make a comparison, we briefly review the procedure of calculating the T-odd TMDs in the spectator model. To do this we expand the gauge link to one-loop order. So the Sivers and Boer-Mulders functions can be computed from

$$\frac{\epsilon_T^{ij} k_{Ti} S_{Tj}}{M} f_{1T}^\perp(x, \mathbf{k}_T^2) = -\frac{1}{4} \frac{1}{(2\pi)^3} \frac{1}{2(1-x)P^+} \text{Tr}[(\mathcal{M}^{(1)}(S)\bar{\mathcal{M}}^{(0)}(S) - \mathcal{M}^{(1)}(-S)\bar{\mathcal{M}}^{(0)}(-S))\gamma^+] + \text{H.c.}, \quad (22)$$

$$\frac{\epsilon_T^{ij} k_{Ti}}{M} h_1^\perp(x, \mathbf{k}_T^2) = \frac{1}{4} \frac{1}{(2\pi)^3} \frac{1}{2(1-x)P^+} \text{Tr}[(\mathcal{M}^{(1)}(S)\bar{\mathcal{M}}^{(0)}(S) + \mathcal{M}^{(1)}(-S)\bar{\mathcal{M}}^{(0)}(-S))i\sigma^{i+}\gamma_5] + \text{H.c.}, \quad (23)$$

where $\mathcal{M}^{(0)}$ and $\mathcal{M}^{(1)}$ are the tree-level and one-loop-level amplitudes of $p \rightarrow qX$ shown in Fig. 1(a). Now, we perform the so-called ‘‘eikonal approximation’’ and take into account only the leading parts of the momenta of the quark after the photon scattering. Therefore, the eikonal propagator of the quark in the light-cone framework in Fig. 1(b) is given by

$$\frac{i(\not{k} + \not{q} - \not{l} + m)}{(k+q-l)^2 - m^2 + i\epsilon} \approx \frac{i(k+q)^-\gamma^+}{-2l^+(k+q)^- + i\epsilon} = \frac{i}{2} \frac{\gamma^+}{-l^+ + i\epsilon}. \quad (24)$$

Then we have the expressions

$$\mathcal{M}^{(0)}(S) = \frac{i(\not{k} - m)}{k^2 - m^2} i g_s(k^2) \frac{1 + \gamma_5 \not{S}}{2} U(P, S), \quad (25)$$

$$\mathcal{M}^{(1)}(S) = \int \frac{d^4 l}{(2\pi)^4} \frac{i^2 e_c^2 \Gamma_{s\rho} n_\rho^\perp (\not{k} - \not{l} + m) i g_s((k-l)^2)}{(l^2 - m_g^2 + i\epsilon)(-l^+ + i\epsilon)((k-l)^2 - m^2 + i\epsilon)((P-k+l)^2 - M_s^2 + i\epsilon)} \frac{1 + \gamma_5 \not{S}}{2} U(P, S), \quad (26)$$

for the scalar diquark, and

$$\mathcal{M}^{(0)}(S) = \frac{i(\not{k} - m)}{k^2 - m^2} \epsilon_\mu^*(P-k, \lambda_a) i \frac{g_a(k^2)}{\sqrt{2}} \gamma^\mu \gamma_5 \frac{1 + \gamma_5 \not{S}}{2} U(P, S), \quad (27)$$

$$\begin{aligned} \mathcal{M}^{(1)}(S) &= \int \frac{d^4 l}{(2\pi)^4} \frac{-i^2 e_c^2 \epsilon_\sigma^*(P-k, \lambda_a) \Gamma_{a\rho}^{\nu\sigma} n_\rho^\perp (\not{k} - \not{l} + m) d_{\mu\nu}}{(l^2 - m_g^2 + i\epsilon)(-l^+ + i\epsilon)((k-l)^2 + i\epsilon)((P-k+l)^2 - M_a^2 + i\epsilon)} i \frac{g_a((k-l)^2)}{\sqrt{2}} \gamma^\mu \gamma_5 \\ &\times \frac{1 + \gamma_5 \not{S}}{2} U(P, S), \end{aligned} \quad (28)$$

for the axial-vector diquark, where

$$\Gamma_{s\rho} = (2P - 2k + l)_\rho, \quad (30)$$

$$\begin{aligned} \Gamma_{a\rho}^{\nu\sigma} &= (2P - 2k + l)_\rho g^{\nu\sigma} - (P - k + (1 + \kappa_a)l)^\sigma g_\rho^\nu \\ &- (P - k - \kappa_a l)^\nu g_\rho^\sigma, \end{aligned} \quad (31)$$

and e_c denotes the color charge of the quark or diquark. κ_a denotes the diquark anomalous chromomagnetic moment. Here we adopt $\kappa_a = 0$.

Integrating over the loop momentum l^μ , we arrive at the analytic expressions for the Sivers function and the Boer-Mulders function contributed by the scalar/axial-vector diquark components,

$$f_{1T}^{\perp(s)}(x, \mathbf{k}_T^2) = h_1^{\perp q(s)}(x, \mathbf{k}_T^2) = -\frac{g_s^2 e_c^2}{4(2\pi)^4} \frac{(1-x)^3 (m+xM)M}{L_s^2(\Lambda_s^2)[\mathbf{k}_T^2 + L_s^2(\Lambda_s^2)]^3}, \quad (32)$$

$$f_{1T}^{\perp(a)}(x, \mathbf{k}_T^2) = \frac{g_a^2 e_c^2}{8(2\pi)^4} \frac{(1-x)^2 x(m+M)M}{L_a^2(\Lambda_a^2)[\mathbf{k}_T^2 + L_a^2(\Lambda_a^2)]^3}, \quad (33)$$

$$h_1^{\perp(a)}(x, \mathbf{k}_T^2) = \frac{g_a^2 e_c^2}{8(2\pi)^4} \frac{(1-x)^2 [(m+(2x-3)M)x-2m]M}{L_a^2(\Lambda_a^2)[\mathbf{k}_T^2 + L_a^2(\Lambda_a^2)]^3}. \quad (34)$$

We can also compute the first transverse moment of the two functions,

$$f_{1T}^{\perp(s)(1)}(x) = h_1^{\perp q(s)(1)}(x) = \int d^2 \mathbf{k}_T \frac{\mathbf{k}_T^2}{2M^2} f_{1T}^{\perp(s)}(x, \mathbf{k}_T^2) = -\frac{g_s^2 e_c^2}{32(2\pi)^3 M} \frac{(m+xM)(1-x)^3}{[L_s^2(\Lambda_s^2)]^2}, \quad (35)$$

$$f_{1T}^{\perp(a)(1)}(x) = \int d^2 \mathbf{k}_T \frac{\mathbf{k}_T^2}{2M^2} f_{1T}^{\perp(a)}(x, \mathbf{k}_T^2) = \frac{g_a^2 e_c^2}{64(2\pi)^3 M} \frac{x(m+M)(1-x)^2}{[L_a^2(\Lambda_a^2)]^2}, \quad (36)$$

$$h_1^{\perp(a)(1)}(x) = \int d^2 \mathbf{k}_T \frac{\mathbf{k}_T^2}{2M^2} h_1^{\perp(a)}(x, \mathbf{k}_T^2) = \frac{g_a^2 e_c^2}{64(2\pi)^3 M} \frac{(1-x)^2 [(m+(2x-3)M)x-2m]}{L_a^2(\Lambda_a^2)^2}. \quad (37)$$

Finally, we apply the following spin-flavor relation to obtain the distributions for the u and d valence quarks [43,58]:

$$f^u = \frac{3}{2} f^{(s)} + \frac{1}{2} f^{(a)}, \quad f^d = f^{(a)}, \quad (38)$$

where f can be f_{1T}^{\perp} or h_1^{\perp} .

B. The quasi-Sivers and quasi-Boer-Mulders functions

Using Eqs. (12) and (13) and Fig. 1, we can calculate the T-odd quasi-TMDs in a similar way. The main difference is the Feynman rules for the eikonal propagator and the eikonal vertex, for which they have the replacements

$$\begin{aligned} \frac{i}{-l^+ + i\epsilon} &\rightarrow \frac{i}{-l_z + i\epsilon}, \\ -ie_c n^\mu &\rightarrow ie_c n_z^\mu. \end{aligned}$$

Then we express $\tilde{\Phi}(x, \mathbf{k}_T, S; P_z)$ as

$$\begin{aligned} \tilde{\Phi}(x, \mathbf{k}_T, S, P_z) &= \frac{1}{(2\pi)^3} \frac{1}{2\lambda} (\mathcal{M}^{(1)}(S) \bar{\mathcal{M}}^{(0)}(S) \\ &\quad \pm \mathcal{M}^{(1)}(-S) \bar{\mathcal{M}}^{(0)}(-S)). \end{aligned} \quad (39)$$

Here, applying a plus or minus sign corresponds to the correlator for the quasi-Sivers function or the quasi-Boer-Mulders function, respectively, λ is deduced from the on-shell condition of the diquark

$$\begin{aligned} \delta((P-k)^2 - M_X^2) &= \delta((P_0 - k_0)^2 - \mathbf{k}_T^2 - (P_z - k_z)^2 - M_X^2) \\ &= \frac{1}{2(P_0 - k_0)} \delta(P_0 - k_0 - \lambda) \end{aligned} \quad (40)$$

and has the expression

$$\lambda = \sqrt{(1-x)^2 P_z^2 + \mathbf{k}_T^2 + M_X^2} = (1-x) P_z \rho_X, \quad (41)$$

with

$$\rho_X = \sqrt{1 + \frac{\mathbf{k}_T^2 + M_X^2}{(1-x)^2 P_z^2}}. \quad (42)$$

Combining the definitions of the quasifunctions in Eqs. (12) and (13) with the correlator (39), it is not difficult to obtain the expressions for the quasi-TMDs,

$$\tilde{f}_{1T}^{\perp(s)}(x, \mathbf{k}_T^2, P_z) = -\frac{g_s(k^2) e_c^2}{4} \frac{1}{(2\pi)^3} \frac{M}{2\lambda} \frac{2\text{Im}\mathcal{I}_1^s}{k^2 - m^2}, \quad (43)$$

$$\tilde{h}_1^{\perp(s)}(x, \mathbf{k}_T^2, P_z) = -\frac{g_s(k^2) e_c^2}{4} \frac{1}{(2\pi)^3} \frac{M}{2\lambda} \frac{2\text{Im}\mathcal{I}_1^{s'}}{k^2 - m^2}, \quad (44)$$

$$\tilde{f}_{1T}^{\perp(a)}(x, \mathbf{k}_T^2, P_z) = \frac{g_a(k^2) e_c^2}{4} \frac{1}{(2\pi)^3} \frac{M}{4\lambda} \frac{2\text{Im}\mathcal{I}_1^a}{k^2 - m^2}, \quad (45)$$

$$\tilde{h}_1^{\perp q(a)}(x, \mathbf{k}_T^2, P_z) = \frac{g_a(k^2) e_c^2}{4} \frac{1}{(2\pi)^3} \frac{M}{4\lambda} \frac{2\text{Im}\mathcal{I}_1^{a'}}{k^2 - m^2}, \quad (46)$$

which are the contributions from the scalar diquark and the axial-vector diquark, respectively, and

$$(\epsilon_T^{ij} \mathbf{k}_{Ti} \mathbf{S}_{Tj}) \mathcal{I}_1^S = \int \frac{d^4 l}{(2\pi)^4} g_s ((k-l)^2) \frac{\text{Tr}[(\not{k} - \not{l} - m)(\not{P} + M) \gamma_5 \not{S} (\not{k} + m)(2P - 2k + l)_\rho n_z^\rho \gamma_z]}{(D_1 + i\epsilon)(D_2 + i\epsilon)(D_3 + i\epsilon)(D_4 + i\epsilon)}, \quad (47)$$

$$-(\epsilon_T^{ij} \mathbf{k}_{Tj}) \mathcal{I}_1^S = \int \frac{d^4 l}{(2\pi)^4} g_s ((k-l)^2) \frac{\text{Tr}[(\not{k} - \not{l} - m)(\not{P} + M) (\not{k} + m)(2P - 2k + l)_\rho n_z^\rho i\sigma_{iz} \gamma_5]}{(D_1 + i\epsilon)(D_2 + i\epsilon)(D_3 + i\epsilon)(D_4 + i\epsilon)}, \quad (48)$$

$$(\epsilon_T^{ij} \mathbf{k}_{Ti} \mathbf{S}_{Tj}) \mathcal{I}_1^a = \int \frac{d^4 l}{(2\pi)^4} g_a ((k-l)^2) \frac{\text{Tr}[(\not{k} - \not{l} + m) \gamma^\mu \gamma_5 (\not{P} + M) \gamma_5 \not{S} \gamma^\alpha \gamma_5 (\not{k} + m) d_{\mu\sigma} d_{\sigma\alpha} \Gamma_{ap}^{\nu\sigma} n_z^\rho \gamma_z]}{(D_1 + i\epsilon)(D_2 + i\epsilon)(D_3 + i\epsilon)(D_4 + i\epsilon)}, \quad (49)$$

$$-(\epsilon_T^{ij} \mathbf{k}_{Tj}) \mathcal{I}_1^a = \int \frac{d^4 l}{(2\pi)^4} g_a ((k-l)^2) \frac{\text{Tr}[(\not{k} - \not{l} + m) \gamma^\mu \gamma_5 (\not{P} + M) \gamma^\alpha \gamma_5 (\not{k} + m) d_{\mu\sigma} d_{\sigma\alpha} \Gamma_{ap}^{\nu\sigma} n_z^\rho i\sigma_{iz} \gamma_5]}{(D_1 + i\epsilon)(D_2 + i\epsilon)(D_3 + i\epsilon)(D_4 + i\epsilon)}, \quad (50)$$

with

$$\begin{aligned} D_1 &= l^2, & D_3 &= (k-l)^2 - m^2, \\ D_2 &= -l^2, & D_4 &= ((P-k+l)^2 - M_s^2). \end{aligned}$$

Similarly, we use the residue theorem and pick up the residues of the diquark propagator and eikonal propagator,

$$\frac{1}{-l^2 + i\epsilon} \rightarrow -2\pi i \delta(l^2), \quad \frac{1}{(P-k+l)^2 - M_X^2 + i\epsilon} \rightarrow -2\pi i \delta((P-k+l)^2 - M_X^2), \quad (51)$$

where the second delta function provides two solutions,

$$\delta((P-k-l)^2 - M_X^2) = \frac{1}{2\lambda_0} (\delta(l_0 + \lambda + \lambda_0) + \delta(l_0 + \lambda - \lambda_0)), \quad (52)$$

with $\lambda_0 = \sqrt{\lambda^2 + \mathbf{l}_T^2 - 2\mathbf{l}_T \cdot \mathbf{k}_T}$. Here the diquark on-shell condition (40) has also been used. For the sake of completeness, both solutions need to be considered.

After computing the traces and the integrals of l_0 and l_z in Eqs. (47)–(50), we have

$$\begin{aligned} \tilde{f}_{1T}^{\perp(s)}(x, \mathbf{k}_T^2, P_z) &= \tilde{h}_1^{\perp q(s)}(x, \mathbf{k}_T^2, P_z) = \frac{1}{(2\pi)^3} \frac{1}{2\rho_s} \frac{e_c^2 g_s^2}{|\mathbf{k}_T^2 + L_s^2(\Lambda_s^2)|^2} M(1-x)^4 \int \frac{d^2 \mathbf{l}_T}{(2\pi)^2} \frac{1}{\lambda_0} \\ &\times \left\{ \frac{(Mk_0 + mP_0) \frac{\mathbf{l}_T \cdot \mathbf{k}_T}{\mathbf{k}_T \cdot \mathbf{k}_T} - M(-\lambda + \lambda_0)}{[(-\lambda + \lambda_0)^2 - \mathbf{l}_T^2][(\mathbf{l}_T - \mathbf{k}_T)^2 + L_s^2(\Lambda_s^2)]^2} + \frac{(Mk_0 + mP_0) \frac{\mathbf{l}_T \cdot \mathbf{k}_T}{\mathbf{k}_T \cdot \mathbf{k}_T} - M(-\lambda - \lambda_0)}{[(-\lambda - \lambda_0)^2 - \mathbf{l}_T^2][(\mathbf{l}_T - \mathbf{k}_T)^2 + L_s^2(\Lambda_s^2)]^2} \right\}, \quad (53) \end{aligned}$$

$$\begin{aligned} \tilde{f}_{1T}^{\perp(a)}(x, \mathbf{k}_T^2, P_z) &= \frac{1}{(2\pi)^3} \frac{1}{4\rho_a} \frac{e_c^2 g_a^2}{|\mathbf{k}_T^2 + L_a^2(\Lambda_a^2)|^2} M(1-x)^3 \int \frac{d^2 \mathbf{l}_T}{(2\pi)^2} \frac{1}{\lambda_0} \\ &\times \left\{ \frac{[(m-3M)k_0 - 2(m-M)xP_0] \frac{\mathbf{l}_T \cdot \mathbf{k}_T}{\mathbf{k}_T \cdot \mathbf{k}_T} + (3M-m)(-\lambda + \lambda_0)}{[(-\lambda + \lambda_0)^2 - \mathbf{l}_T^2][(\mathbf{l}_T - \mathbf{k}_T)^2 + L_a^2(\Lambda_a^2)]^2} \right. \\ &\left. + \frac{[(m-3M)k_0 - 2(m-M)xP_0] \frac{\mathbf{l}_T \cdot \mathbf{k}_T}{\mathbf{k}_T \cdot \mathbf{k}_T} + (3M-m)(-\lambda - \lambda_0)}{[(-\lambda - \lambda_0)^2 - \mathbf{l}_T^2][(\mathbf{l}_T - \mathbf{k}_T)^2 + L_a^2(\Lambda_a^2)]^2} \right\}, \quad (54) \end{aligned}$$

$$\begin{aligned} \tilde{h}_1^{\perp(a)}(x, \mathbf{k}_T^2, P_z) &= \frac{1}{(2\pi)^3} \frac{1}{4\rho_a} \frac{e_c^2 g_a^2}{|\mathbf{k}_T^2 + L_a^2(\Lambda_a^2)|^2} M(1-x)^3 \int \frac{d^2 \mathbf{l}_T}{(2\pi)^2} \frac{1}{\lambda_0} \\ &\times \left\{ \frac{[-(m+M(2x-3))k_0 + 2mP_0] \frac{\mathbf{l}_T \cdot \mathbf{k}_T}{\mathbf{k}_T \cdot \mathbf{k}_T} + (m+M(2x-3))(-\lambda + \lambda_0)}{[(-\lambda + \lambda_0)^2 - \mathbf{l}_T^2][(\mathbf{l}_T - \mathbf{k}_T)^2 + L_a^2(\Lambda_a^2)]^2} \right. \\ &\left. + \frac{[-(m+M(2x-3))k_0 + 2mP_0] \frac{\mathbf{l}_T \cdot \mathbf{k}_T}{\mathbf{k}_T \cdot \mathbf{k}_T} + (m+M(2x-3))(-\lambda - \lambda_0)}{[(-\lambda - \lambda_0)^2 - \mathbf{l}_T^2][(\mathbf{l}_T - \mathbf{k}_T)^2 + L_a^2(\Lambda_a^2)]^2} \right\}. \quad (56) \end{aligned}$$

The integration over L_T can be performed numerically. With the above results, we can obtain the quasi-Sivers function and the quasi-Boer-Mulders function of the u and d quarks using the relation similar to Eq. (38),

$$\tilde{f}^u = \frac{3}{2}\tilde{f}^{(s)} + \frac{1}{2}\tilde{f}^{(a)}, \quad \tilde{f}^d = \tilde{f}^{(a)}. \quad (57)$$

We can also provide the first transverse moment of these quasifunctions,

$$\tilde{f}_{1T}^{\perp(1)}(x, P_z) = \int d^2k_T \frac{k_T^2}{2M^2} \tilde{f}_{1T}^{\perp q}(x, k_T^2, P_z), \quad (58)$$

$$\tilde{h}_1^{\perp(1)}(x, P_z) = \int d^2k_T \frac{k_T^2}{2M^2} \tilde{h}_1^{\perp q}(x, k_T^2, P_z). \quad (59)$$

Finally, we find that the T-odd TMDs reduce to the standard TMDs in the limit $P_z \rightarrow \infty$,

$$\tilde{f}_{1T}^{\perp q}(x, k_T^2, P_z \rightarrow \infty) = f_{1T}^{\perp q}(x, k_T^2), \quad (60)$$

$$\tilde{h}_1^{\perp q}(x, k_T^2, P_z \rightarrow \infty) = h_1^{\perp q}(x, k_T^2). \quad (61)$$

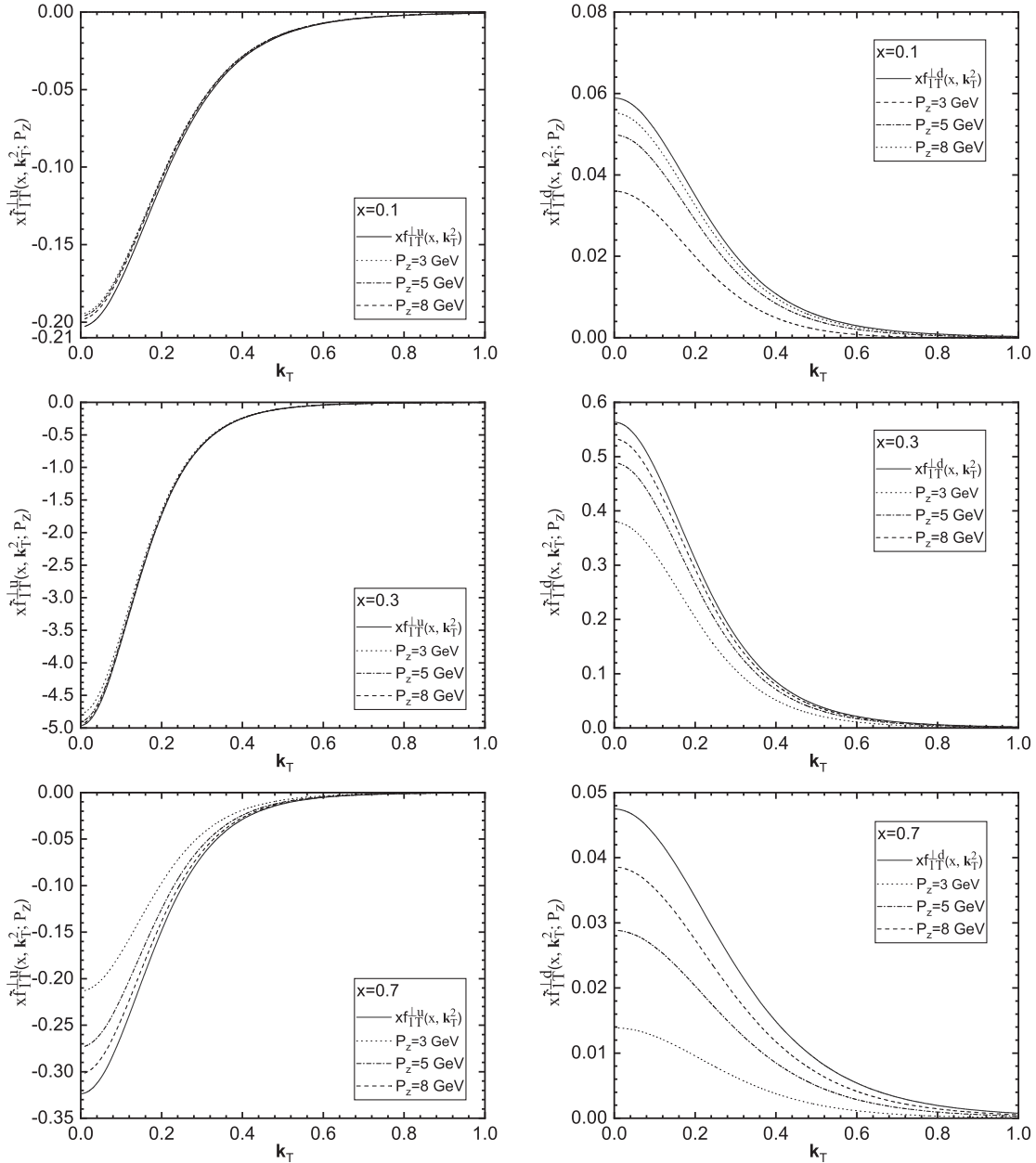


FIG. 2. The quasi-Sivers function $\tilde{f}_{1T}^{\perp q}(x, k_T^2; P_z)$ (multiplied by x) of the up (left) and down (right) quarks as a function of k_T in the spectator model. The dotted line, dot-dashed line, and dashed line correspond to the results at $P_z = 3, 5,$ and 8 GeV, respectively.

This extends the observation that the quasi-PDFs should reduce to the standard PDFs defined in terms of the light-cone correlation functions [5,59] at $P_z \rightarrow \infty$.

IV. NUMERICAL RESULT

In this section, we will numerically compute the T-odd quasi-TMDs of u and d quarks to study the P_z dependence of these distributions and compare them with the standard distributions. To do this we need to assign the values of the parameters in Eqs. (53)–(56). Here we adopt the choices in the original works [43,58],

$$\begin{aligned}
 m &= 0.36 \text{ GeV}, & g_s^2 &= 6.525, & g_a^2 &= 28.716, & (62) \\
 \Lambda_{s/a} &= 0.5 \text{ GeV}, & M_s &= 0.6 \text{ GeV}, & M_a &= 0.8 \text{ GeV}. & (63)
 \end{aligned}$$

The factors g_s and g_a are determined from the normalization condition of the unpolarized distributions,

$$\begin{aligned}
 \pi \int_0^1 dx \int_0^\infty dk_T^2 f_1^{(s)}(x, k_T^2) &= 1, \\
 \pi \int_0^1 dx \int_0^\infty dk_T^2 f_1^{(a)}(x, k_T^2) &= 1, & (64)
 \end{aligned}$$

which consequently normalizes f_1^u to 2 and f_1^d to 1.

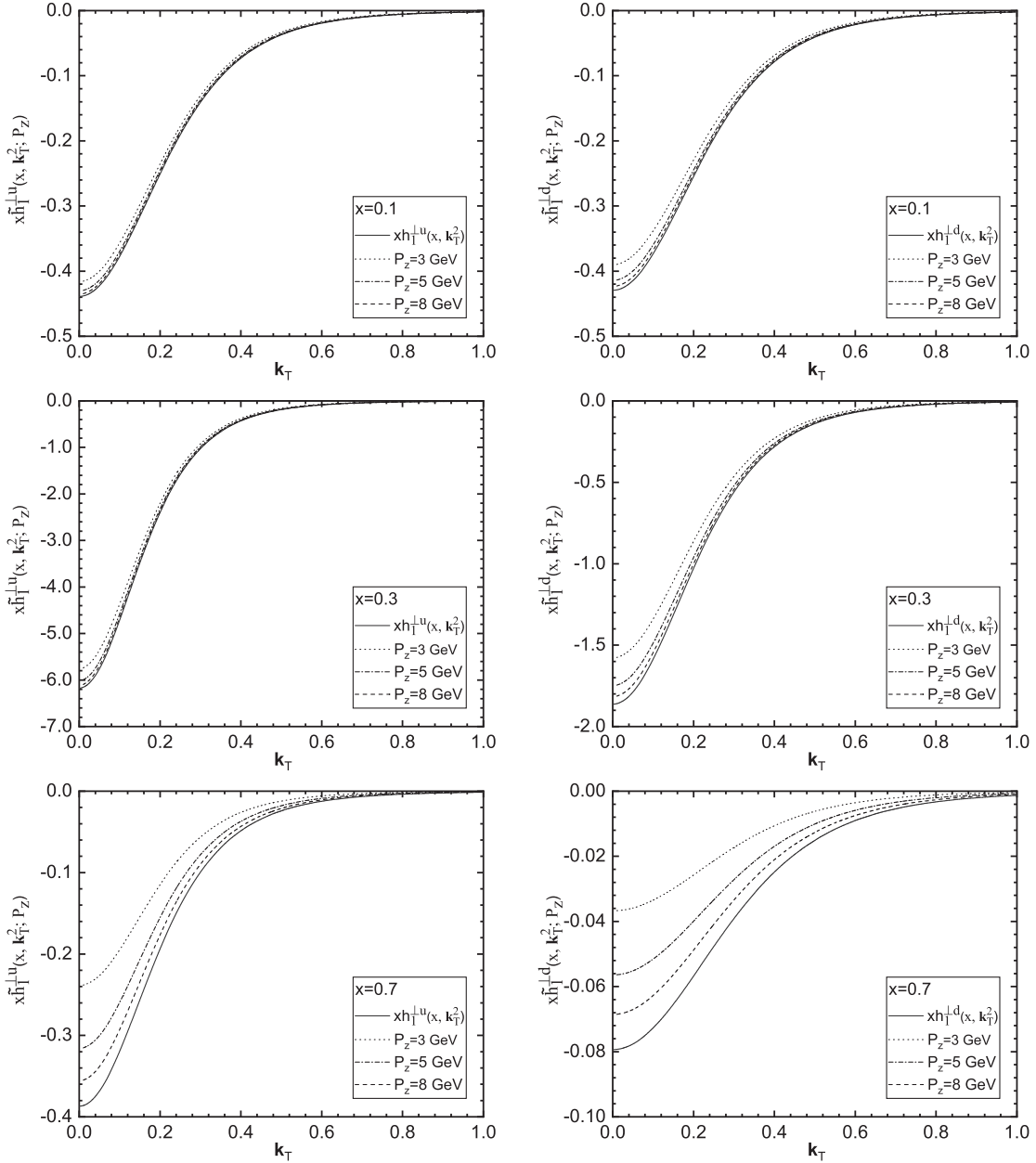


FIG. 3. The $x\tilde{f}_{1T}^{\perp(1)u/d}(x, P_z, k_T^2)$ and $x\tilde{h}_{1T}^{\perp(1)u/d}(x, P_z, k_T^2)$ at $P_z = 3, 5,$ and 8 GeV in the spectator model. The upper, central, and lower rows show the results at $x = 0.1, 0.3, 0.7,$ respectively.

In order to replace the Abelian interaction of gluons with the QCD color interaction, we make the following replacement [47]:

$$\frac{e_c^2}{4\pi} \rightarrow C_F \alpha_s, \quad (65)$$

where $C_F = 4/3$ and we choose $\alpha_s \approx 0.3$ in the calculation.

In Fig. 2, we plot the quasi-Sivers function (timed with x) $\tilde{f}_{1T}^\perp(x, \mathbf{k}_T^2; P_z)$ of the up (left panel) and down (right panel) quarks as a function of $k_T = |\mathbf{k}_T|$. The upper, central, and lower panels show the results at $x = 0.1, 0.3,$ and 0.7 , respectively. The dotted line, the dot-dashed line and the dashed line correspond to the results at $P_z = 3, 5,$ and 8 GeV, respectively. The solid line shows the result of the standard Sivers function $f_{1T}^\perp(x, \mathbf{k}_T^2)$ for comparison. The quasi-Boer-Mulders function (timed with x) $\tilde{h}_1^\perp(x, \mathbf{k}_T^2; P_z)$ is plotted in Fig. 3 in a similar way. One can find that the sizes of the quasi-TMDs decrease with increasing k_T , which is similar to the k_T -shape of the standard TMDs. The results also show that the quasi-Sivers function of the up quark is negative, while that of the down quark is positive. The quasi-Boer-Mulders functions of the up and down quarks are both negative. In all cases, the sizes of the

T-odd quasi-TMDs are smaller than those of the standard TMDs. However, as P_z increases, the sizes of the quasi-TMDs increase and converge to the standard TMDs. Another observation is that the convergence depends on x ; that is, in the smaller x region, in general the quasi-TMDs converge more quickly as P_z increases.

In the upper panel of Fig. 4, we plot the x dependence of the first transverse moment of the quasi-Sivers function $\tilde{f}_{1T}^{\perp(1)}(x, P_z)$ (timed with x) of the u (left panel) and d (right panel) quarks defined in Eq. (58). The dotted line, the dot-dashed line, and the dashed line correspond to $P_z = 3, 5,$ and 8 GeV, respectively. The solid line denotes the first transverse moment of the standard Sivers function $f_{1T}^{\perp(1)}(x)$. Similarly, we plot the x dependence of the first transverse moment of the quasi-Boer-Mulders function $\tilde{h}_1^{\perp(1)}(x, P_z)$ (timed with x) of the u (left panel) and d (right panel) quarks in the lower panel of Fig. 4. Again, here the solid line denotes the first transverse moment of the standard Boer-Mulders function. We note that our results of $f_{1T}^{\perp(1)}(x)$ and $h_1^{\perp(1)}(x)$ are qualitatively consistent with the phenomenologically extractions in size and sign. We find that as P_z increases, in general, the sizes of $\tilde{f}_{1T}^{\perp(1)}(x, P_z)$ and

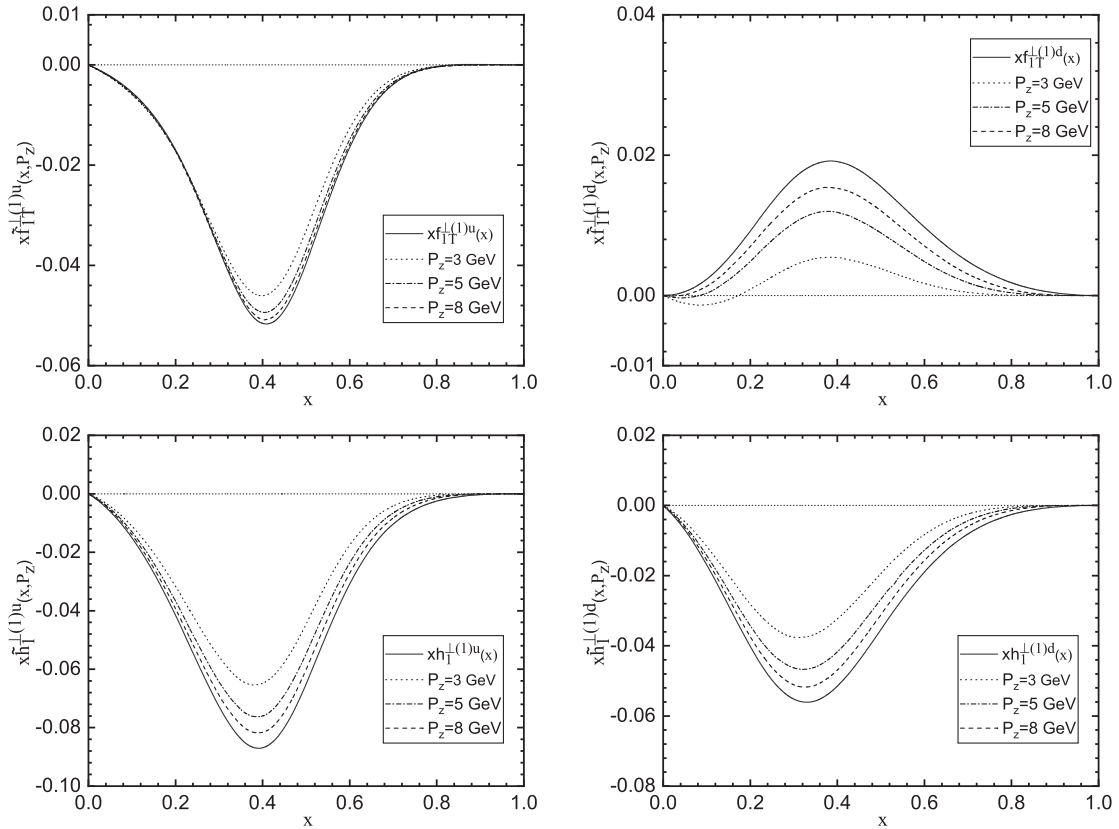


FIG. 4. The first k_T -moment of the quasi-Sivers function $x\tilde{f}_{1T}^{\perp(1)q}(x, P_z)$ (upper) and that of the quasi-Boer-Mulders function $x\tilde{h}_1^{\perp(1)q}(x, P_z)$ (lower) as a function of x in the spectator model. The dotted, dash-dotted, and dashed lines denote the results at $P_z = 3, 5,$ and 8 GeV, respectively. The solid lines depict the corresponding first k_T -moment of the standard functions.

$\tilde{h}_1^{\perp(1)}(x, P_z)$ increase and the shapes of them get close to the corresponding standard distributions. There are also some exceptions which can be seen in the small x region of the quasi-Sivers function, particularly, for the d quark the quasifunction can have a sign opposite to that of the standard function in the small region. Also a node appears at $x \approx 0.2$ for $\tilde{f}_{1T}^{\perp(1)d}(x, P_z)$ at the small P_z region.

To provide a more comprehensive discussion on the variation of the quasidistributions with increasing P_z in different x regions, in Fig. 5 we plot the ratios $\tilde{f}_{1T}^{\perp(1)}(x, P_z)/f_{1T}^{\perp(1)}(x)$ (upper panel) and $\tilde{h}_1^{\perp(1)}(x, P_z)/h_1^{\perp(1)}(x)$ (lower panel) as functions of P_z at fixed $x = 0.1, 0.3, 0.5,$ and 0.7 , respectively. From the figure one can see that the ratio $\tilde{f}_{1T}^{\perp(1)}(x, P_z)/f_{1T}^{\perp(1)}(x)$ is clearly flavor dependent. For the u quark Sivers distribution the ratio is less than 1 except $x = 0.1$; the ratios in different x regions are positive approaches to 1 around $P_z \approx 8$ GeV. Meanwhile, for the d quark Sivers function, the ratio is negative in the smaller P_z region and turns to be positive in the larger P_z region. Also, the ratio $\tilde{f}_{1T}^{\perp(1)}(x, P_z)/f_{1T}^{\perp(1)}(x)$ for the d quark converges to 1 slower than that for the u quark distribution. In the case of the Boer-Mulders function, the ratios for the u quark and the

d quark are very similar; that is, they are positive and less than 1 in the entire x region. In the region $x < 0.5$, the ratio approaches 0.9–0.95 at $P_z = 8$ GeV, while in the larger x region (such as $x = 0.7$) the ratio approaches 0.8–0.85 at $P_z = 8$ GeV. That is, in the large x region the quasi-Boer-Mulders function converges slower.

Compared with the results in Ref. [33], we can find that there are some common features shared by the T-odd quasi-TMDs and the T-even quasi-PDFs. First, in both cases the quasidistributions reduce to the standard distributions in the limit $P_z \rightarrow \infty$. Second, the quasidistributions can have an opposite sign to the standard distributions in certain regions, such as $\tilde{f}_{1T}^{\perp d}(x, k_T^2; P_z)$, $\tilde{g}_1^d(x, P_z)$, and $\tilde{h}_1^u(x, P_z)$. However, there is also the feature of the T-odd quasi-TMDs which is different from that of T-even quasi-PDFs. As is evident from Ref. [33], for the intermediate x region $0.1 < x < 0.4$ – 0.5 , the quasi-PDFs $\tilde{f}_1^q(x)$, $\tilde{g}_1^q(x)$, and $\tilde{h}_1^q(x)$ approximate the corresponding standard PDFs within 20%–30% when $P_z \geq 1.5$ – 2 GeV. While from Fig. 5 we find that the T-odd quasi-TMDs in the spectator model are fair approximations to the standard TMDs (within 20%–30%) in the intermediate x region when $P_z \geq 2.5$ – 3 GeV, which is larger than the case of the

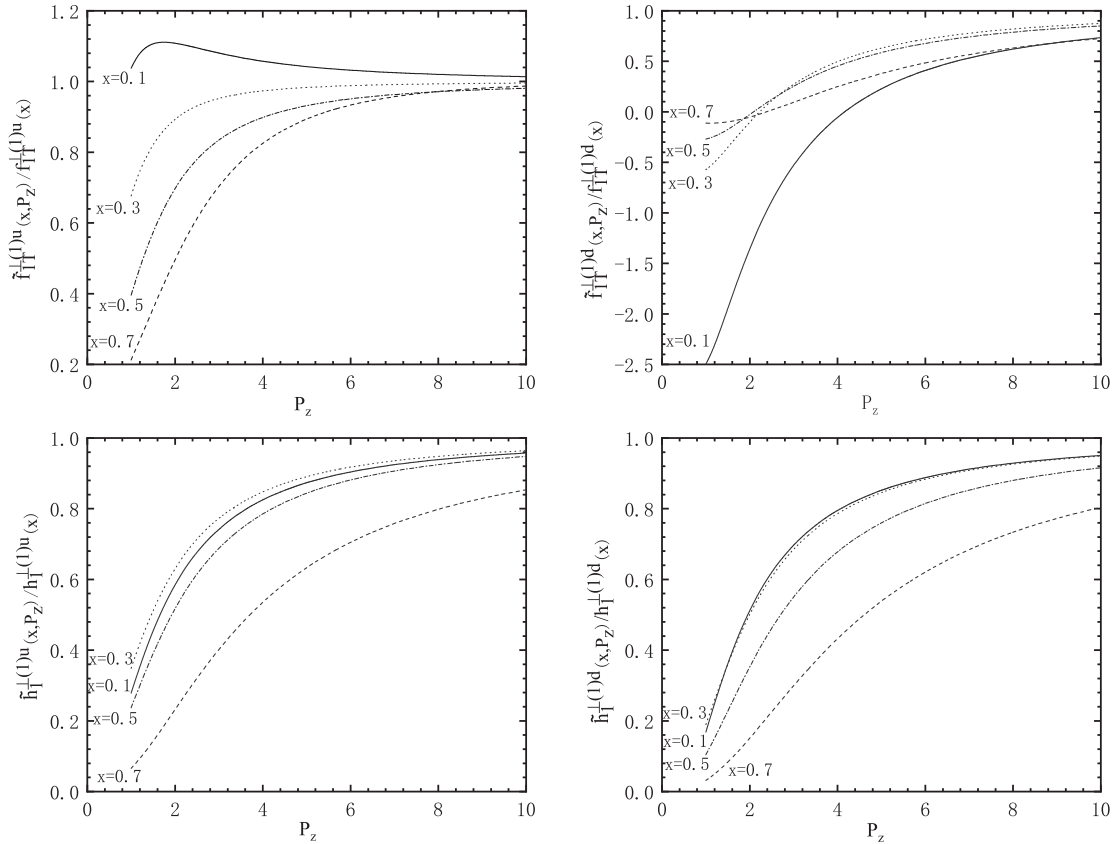


FIG. 5. Upper: the ratio of $\tilde{f}_{1T}^{\perp(1)}(x, P_z)/f_{1T}^{\perp(1)}(x)$ as a function of P_z for the u and d quarks in the spectator model. Lower: the ratio $\tilde{h}_1^{\perp(1)}(x, P_z)/h_1^{\perp(1)}(x)$ as a function of P_z for the u and d quarks. The solid, dotted, dash-dotted, and dashed lines correspond to the results at $x = 0.1, 0.3, 0.5,$ and 0.7 , respectively.

T-even quasi-PDFs. Thus, to obtain the results for the T-odd TMDs as accurate as that for the T-even PDFs in the lattice calculation, one should explore a relatively larger P_z region. Finally, in our study we have chosen the diquark anomalous chromomagnetic moment as $\kappa_a = 0$ to simplify the calculation. We find that varying κ_a between 0 and 1 will not change our numerical result qualitatively. Particularly, in the case $\kappa_a = 1$ there is still a fair agreement between the quasi-TMDs and the standard TMDs in the region $P_z \geq 2-3$ GeV.

V. SUMMARY

In this paper, we computed the two twist-2 T-odd quasidistributions, the quasi-Sivers function $\tilde{f}_{1T}^\perp(x, \mathbf{k}_T^2, P_z)$ and the quasi-Boer-Mulders function $\tilde{h}_1^\perp(x, \mathbf{k}_T^2, P_z)$, in a spectator model with both scalar diquark and axial-vector diquark. The quasifunctions are obtained by replacing γ^+ and σ^{i+} with γ_z and σ_{iz} , which make them defined in a four-dimensional Euclidean space rather than in the Minkowski space-time. We applied the dipolar form factor for the proton-quark-diquark vertex to provide the expressions of the quasifunctions and compare them with the standard functions in the same model. To perform the integrations over the l_0 and l_z components of the gluon four-momentum, we adopted the cut-diagram approach. We found that the two T-odd quasi-TMDs reduce to the analytical results of the corresponding standard TMDs in the limit $P_z \rightarrow \infty$, which is analogous to the results of the

T-even quasi-PDFs \tilde{f}_1 , \tilde{g}_1 , and \tilde{h}_1 . This observation is also supported by the numerical results for $\tilde{f}_{1T}^\perp(x, \mathbf{k}_T^2; P_z)$ and $\tilde{h}_1^\perp(x, \mathbf{k}_T^2; P_z)$ as functions of the transverse momentum k_T at different x and P_z . Another observation is that the convergence depends on x ; that is, in general the quasi-TMDs approach the standard ones more quickly in the smaller x region than in the larger x region as P_z increases. We studied the flavor dependence of the quasi-TMDs and found that the quasi-Sivers functions of the u and d quarks are quite different, while the quasi-Boer-Mulders functions are almost flavor blind. We also calculated the first k_T -moment of the T-odd quasi-TMDs $\tilde{f}_{1T}^{\perp(1)}(x, P_z)$ and $\tilde{h}_1^{\perp(1)}(x, P_z)$ as functions of x and P_z . We found that $\tilde{f}_{1T}^{\perp(1)}(x, P_z)$ and $\tilde{h}_1^{\perp(1)}(x, P_z)$ in the spectator model are fair approximations to the standard ones (within 20%–30%) in the region $0.1 < x < 0.5$ when $P_z \geq 2.5-3$ GeV. This is in general larger than the value of the T-even quasi-PDFs $\tilde{f}_1^q(x)$, $\tilde{g}_1^q(x)$, and $\tilde{h}_1^q(x)$. In summary, our study has provided model implications and constraints on the quasi-Sivers function and the quasi-Boer-Mulders function, and it is possible to access the T-odd standard distributions from lattice QCD calculations in the region $P_z > 2.5$ GeV as fair approximations.

ACKNOWLEDGMENTS

This work is partially supported by the National Natural Science Foundation of China under Grant No. 12150013.

-
- [1] A. Bacchetta, M. Diehl, K. Goeke, A. Metz, P.J. Mulders, and M. Schlegel, *J. High Energy Phys.* **02** (2007) 093.
 - [2] D. W. Sivers, *Phys. Rev. D* **41**, 83 (1990); **43**, 261 (1991).
 - [3] M. Anselmino, M. Boglione, J. C. Collins, U. D'Alesio, A. V. Efremov, K. Goeke, A. Kotzinian, S. Menzel, A. Metz, F. Murgia *et al.*, arXiv:hep-ph/0511017.
 - [4] D. Boer and P.J. Mulders, *Phys. Rev. D* **57**, 5780 (1998).
 - [5] X. Ji, *Phys. Rev. Lett.* **110**, 262002 (2013).
 - [6] X. Ji, *Sci. China Phys. Mech. Astron.* **57**, 1407 (2014).
 - [7] H. W. Lin, J. W. Chen, S. D. Cohen, and X. Ji, *Phys. Rev. D* **91**, 054510 (2015).
 - [8] C. Alexandrou, K. Cichy, V. Drach, E. Garcia-Ramos, K. Hadjiyiannakou, K. Jansen, F. Steffens, and C. Wiese, *Phys. Rev. D* **92**, 014502 (2015).
 - [9] C. Alexandrou, K. Cichy, M. Constantinou, K. Hadjiyiannakou, K. Jansen, F. Steffens, and C. Wiese, *Phys. Rev. D* **96**, 014513 (2017).
 - [10] J. W. Chen, S. D. Cohen, X. Ji, H. W. Lin, and J. H. Zhang, *Nucl. Phys.* **B911**, 246 (2016).
 - [11] J. H. Zhang, J. W. Chen, X. Ji, L. Jin, and H. W. Lin, *Phys. Rev. D* **95**, 094514 (2017).
 - [12] J. H. Zhang, J.-W. Chen, L. Jin, H.-W. Lin, A. Schäfer, P. Sun, Y.-B. Yang, J.-H. Zhang, and Y. Zhao (LP3 Collaboration), *Nucl. Phys.* **B939**, 429 (2019).
 - [13] C. Alexandrou, K. Cichy, M. Constantinou, K. Hadjiyiannakou, K. Jansen, H. Panagopoulos, and F. Steffens, *Nucl. Phys.* **B923**, 394 (2017).
 - [14] J. W. Chen, T. Ishikawa, L. Jin, H. W. Lin, Y. B. Yang, J. H. Zhang, and Y. Zhao, *Phys. Rev. D* **97**, 014505 (2018).
 - [15] J. Green, K. Jansen, and F. Steffens, *Phys. Rev. Lett.* **121**, 022004 (2018).
 - [16] H. W. Lin, J.-W. Chen, T. Ishikawa, and J.-H. Zhang (LP3 Collaboration), *Phys. Rev. D* **98**, 054504 (2018).
 - [17] K. Orginos, A. Radyushkin, J. Karpie, and S. Zafeiropoulos, *Phys. Rev. D* **96**, 094503 (2017).
 - [18] G. S. Bali *et al.*, *Eur. Phys. J. C* **78**, 217 (2018).
 - [19] C. Alexandrou, S. Bacchio, K. Cichy, M. Constantinou, K. Hadjiyiannakou, K. Jansen, G. Koutsou, A. Scapellato, and F. Steffens, *EPJ Web Conf.* **175**, 14008 (2018).
 - [20] J. W. Chen *et al.*, *Nucl. Phys.* **B939**, 429 (2019).
 - [21] C. Alexandrou, K. Cichy, M. Constantinou, K. Jansen, A. Scapellato, and F. Steffens, *Phys. Rev. Lett.* **121**, 112001 (2018).

- [22] J. W. Chen, L. Jin, H. W. Lin, Y. S. Liu, Y. B. Yang, J. H. Zhang, and Y. Zhao, [arXiv:1803.04393](#).
- [23] C. Alexandrou, K. Cichy, M. Constantinou, K. Jansen, A. Scapellato, and F. Steffens, *Phys. Rev. D* **98**, 091503 (2018).
- [24] Y. S. Liu, J. W. Chen, L. Jin, H. W. Lin, Y. B. Yang, J. H. Zhang, and Y. Zhao, *Phys. Rev. D* **101**, 034020 (2020).
- [25] G. S. Bali, V. M. Braun, B. Gläsel, M. Göckeler, M. Gruber, F. Hutzler, P. Korcyl, A. Schäfer, P. Wein, and J. H. Zhang, *Phys. Rev. D* **98**, 094507 (2018).
- [26] H. W. Lin, J. W. Chen, L. Jin, Y. S. Liu, Y. B. Yang, J. H. Zhang, and Y. Zhao, *Phys. Rev. Lett.* **121**, 242003 (2018).
- [27] Y. S. Liu *et al.* (Lattice Parton Collaboration), *Phys. Rev. D* **101**, 034020 (2020).
- [28] X. Ji, L. C. Jin, F. Yuan, J. H. Zhang, and Y. Zhao, *Phys. Rev. D* **99**, 114006 (2019).
- [29] M. A. Ebert, I. W. Stewart, and Y. Zhao, *J. High Energy Phys.* **09** (2019) 037.
- [30] X. Ji, Y. S. Liu, Y. Liu, J. H. Zhang, and Y. Zhao, *Rev. Mod. Phys.* **93**, 035005 (2021).
- [31] M. A. Ebert, S. T. Schindler, I. W. Stewart, and Y. Zhao, *J. High Energy Phys.* **09** (2020) 099.
- [32] X. Ji, Y. Liu, A. Schäfer, and F. Yuan, *Phys. Rev. D* **103**, 074005 (2021).
- [33] L. Gamberg, Z. B. Kang, I. Vitev, and H. Xing, *Phys. Lett. B* **743**, 112 (2015).
- [34] A. Bacchetta, M. Radici, B. Pasquini, and X. Xiong, *Phys. Rev. D* **95**, 014036 (2017).
- [35] S. i. Nam, *Mod. Phys. Lett. A* **32**, 1750218 (2017).
- [36] W. Broniowski and E. Ruiz Arriola, *Phys. Lett. B* **773**, 385 (2017).
- [37] T. J. Hobbs, *Phys. Rev. D* **97**, 054028 (2018).
- [38] W. Broniowski and E. Ruiz Arriola, *Phys. Rev. D* **97**, 034031 (2018).
- [39] S. S. Xu, L. Chang, C. D. Roberts, and H. S. Zong, *Phys. Rev. D* **97**, 094014 (2018).
- [40] H. D. Son, A. Tandogan, and M. V. Polyakov, *Phys. Lett. B* **808**, 135665 (2020).
- [41] Z. Lu and B. Q. Ma, *Nucl. Phys.* **A741**, 200 (2004).
- [42] Z. B. Kang, J. W. Qiu, and H. Zhang, *Phys. Rev. D* **81**, 114030 (2010).
- [43] A. Bacchetta, A. Schaefer, and J. J. Yang, *Phys. Lett. B* **578**, 109 (2004).
- [44] S. Bhattacharya, C. Cocuzza, and A. Metz, *Phys. Lett. B* **788**, 453 (2019).
- [45] S. Bhattacharya, C. Cocuzza, and A. Metz, *Phys. Rev. D* **102**, 054021 (2020).
- [46] Z. L. Ma, J. Q. Zhu, and Z. Lu, *Phys. Rev. D* **101**, 114005 (2020).
- [47] S. J. Brodsky, D. S. Hwang, and I. Schmidt, *Phys. Lett. B* **530**, 99 (2002).
- [48] D. Boer, S. J. Brodsky, and D. S. Hwang, *Phys. Rev. D* **67**, 054003 (2003).
- [49] L. P. Gamberg, G. R. Goldstein, and K. A. Oganessyan, *Phys. Rev. D* **67**, 071504 (2003).
- [50] Z. Lu and B. Q. Ma, *Phys. Rev. D* **70**, 094044 (2004).
- [51] L. P. Gamberg, G. R. Goldstein, and M. Schlegel, *Phys. Rev. D* **77**, 094016 (2008).
- [52] A. Bacchetta, F. Conti, and M. Radici, *Phys. Rev. D* **78**, 074010 (2008).
- [53] B. Pasquini and F. Yuan, *Phys. Rev. D* **81**, 114013 (2010).
- [54] A. Courtoy, F. Fratini, S. Scopetta, and V. Vento, *Phys. Rev. D* **78**, 034002 (2008).
- [55] A. Courtoy, S. Scopetta, and V. Vento, *Phys. Rev. D* **80**, 074032 (2009).
- [56] F. Yuan, *Phys. Lett. B* **575**, 45 (2003).
- [57] A. Courtoy, S. Scopetta, and V. Vento, *Phys. Rev. D* **79**, 074001 (2009).
- [58] R. Jakob, P. J. Mulders, and J. Rodrigues, *Nucl. Phys.* **A626**, 937 (1997).
- [59] Y. Q. Ma and J. W. Qiu, *Phys. Rev. D* **98**, 074021 (2018).